Mathematical Model of a Multi-link Surgical Manipulator Joint with an Antiseptic Coating

Ryszard Leniowski, Lucyna Leniowska

Abstract:

We present a synthesis of the mathematical model of a joint of a new generation multi-link surgical micromanipulator. A design of such a device involves finding solutions for several difficult problems which do not appear in classical 'large' robots. A prototype in development has six links, and it is driven by brushless servomotors with planetary and worm gears, for which the total transmission ratio is above 10000:1. Most importantly, whole construction is covered by an antiseptic coating which substantially changes manipulator's dynamics. Because of the complicated form of the drive model with three-stage planetary gearings and coating interactions, control of such system is significantly different from control of a typical industrial robot. This paper presents a synthesis of the model of the joint, which can be used to design the control system. In this work the derived model is used to examine joint's properties and characteristics. Results are presented graphically and discussed.

Keywords: *surgical manipulators, mathematical modeling, coating interactions.*

1. Introduction

A design of new generation multi-link surgical micromanipulators is connected with finding solutions of several difficult problems which do not appear in classical "big" robots. They concern the robot construction and its assembly as well as the control system design. An example of such construction is the model of a multi-link surgical manipulator which was designed within the scope of the project from the Ministry of Science and Higher Education No 2376/B/T02/2010/38. The manipulators' prototype contains 6 links with diameter of 8-10 mm and with the length of the modules about 130 mm. It is driven by brushless servomotors with planetary and worm gears, for which the total transmission ratio is above 10000:1. Essential feature of this manipulator is an antiseptic coating which covers all the construction.

The manipulator in question belongs to the group of miniature robots (a working space has a cubic capacity less than 1 dcm^3). The vital feature to distinguish the miniature robot constructions from their macro counterpart is substantially low efficiency of the whole driving path. For currently existing, the most perfect devices, the efficiency is about 45-50% (for motors) and 50-55% (the multi-stages planetary gearing). For comparison, the "macro" robots efficiency is approximately 90-93% (motors) and 78-86% (gearing). However, the construction of miniature harmonic drive gearing with a big reduction ratio and diameter not greater than 5 mm is still not available.

Low efficiency of the driving path (with reference to the generated torque) is caused by high friction occurred in motors and gearings. The other feature which differ the described multi-link robot from similar well-known constructions is the aforementioned antiseptic coating. It covers the outer surface of manipulator and in this way insulates all parts of construction from a human body providing a high sterility. During robots movement (bending and twisting), the coating generates some complex dynamic interactions acting on the joints. For those reasons model of joints dynamics is more complex than corresponding one for the "macro" robot constructions. In consequence it influences robot precision and also the design and implementation of control system is more complicated.

This paper presents the synthesis of a mathematical model of the multi-link surgical manipulator joint with an antiseptic coating. The main aim of the work is to investigate with the use of simulation methods some characteristics and properties of joint in question. In this way it might be possible to answer on the following question: is it feasible that position accuracy for the manipulator in spite of complex drives dynamics in the miniature construction can be less than assumed level of 0.5 mm? To do this, it is important to build an appropriate model with special attention paid to the induction of vibration. These data will help in fitting the best method for model parameters identification and allow designing an accurate and saving control system. Additionally, the joint model is also a part of virtual simulator, which is currently developed for investigation and training purposes. In first approach, it will be used for designing of control system.

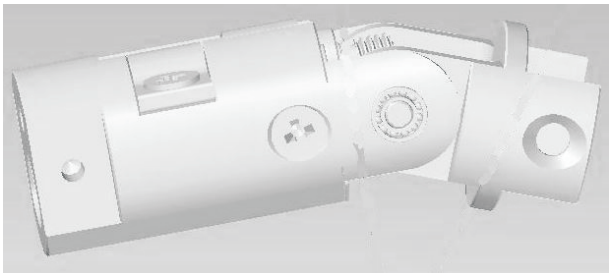

Fig. 1. View of the joint.

The joint model (Fig. 1) consists of following elements: the planetary and worm gears, the brushless motor (BLDC) and the antiseptic coating. Separation of components in the model enables a better configuration of the structure, so that the described prototype can be characterized by high-tech parameters. Currently, the prototype

design of medical robot is based on the sub-assemblies from the Faulhaber [3] company. It is obvious, that they can be replaced by the better ones if such will be accessible in the future.

2. Planetary gearing model

Considering disturbing torques acting on the joint in question it can be noticed that the biggest contribution belongs to the multi-stage planetary gearing. It is the reason, why understanding and recognition of its model is so important for designing of the control system. In recent years (2007-2009) some very accurate models of planetary gearings have been worked out [4]. They has form of matrix differential equation of second order and dimensions: $6N \times 6N$, $N = (3 + p)$, where p is a number of planets. Unfortunately, in the cited paper, the description of friction is omitted because of its complexity. For $p = 4$, inertia and stiffness matrixes dimensions are (42×42) and they generate some of resonance frequencies. On the base of [4] it can be noticed that they consist three groups of frequencies. Regarding only low and middle resonance frequencies, the initial model can be replaced with reduced model, containing three spinning masses as follows:

$$\begin{aligned} J_m q_m + F_m q_m &= T_m q - \eta_1 T_{g1} \\ T_{g1} &= k_{11}\, \eta_1 q_m - q_{g1} + k_{31}\, \eta_1 q_m - q_{g1}^3 \\ J_{g1} q_1 + F_{g1} q_{g1} &= T_{g1} - \eta_2 T_{g2} \\ T_{g2} &= k_{12}\, \eta_2 q_{g1} - q_{g2} + k_{32}\, \eta_2 q_{g1} - q_{g2}^3 \\ J_{g2} q_2 + F_{g2} q_{g2} &= T_{g2} - T_l \end{aligned} \tag{1}$$

where: J_m is the motor inertia; J_{g1} and J_{g2} – the inertias of rotating gears; T_{g1} and T_{g2} – the non-linear torque springs interactions; F_m, F_{g1}, F_{g2} – the friction torques; T_m – the driven torque; T_l – the arms loading torque; η_1, η_2 – the two-stage gear ratios. Because of existing in eq. (1) nonlinear torque springs interactions, the presented model is very close to real conditions.

The essential component of eq. (1) are the friction torques. A phenomenon existing in all mechanical devices having any moving parts, friction can be observed as reaction forces/torques acting on the contact surfaces of two bodies. Its mathematical models currently in use can be classified into two categories. The first contains so called classical models of friction which are limited to static characteristics. The second category includes the modern models which try to take into account also the dynamics of this complex phenomenon. Such dynamical models, based on differential equations are usually results of empirical research not rarely originated from very loosely connected branches of science (e.g. mechanics and geophysics). Considering some new models of friction, the simplicity and realism of "LuGre" [5] makes it worthy of attention. It describes the friction force as a fibre interaction fastened between rubbed surfaces and treats fibres as viscoelastic. The friction torque reaction (F_m, F_{g1}, F_{g2}) contains three components:

$$F = \sigma_0 z + \sigma_1 z + \sigma_2 v \tag{2}$$

where

$$\frac{dz}{dt} = v - \sigma_0 \frac{|v|}{gv} z, \quad gv = \alpha_0 + \alpha_1 e^{-(v/v_0)^2} \tag{3}$$

Parameters σ_0, σ_1 and σ_2 denote the fibre stiffness, the fibre damping and the viscous coefficient accordingly. Coefficients α_0 and α_1 model the shape of function, $g\,v$ and v is the related velocity of rubbed surfaces. Non-linear differential equation (3), together with the function $g(v)$, establishes the "system with memory" which permits for better modelling of real processes. Equations (2) and (3) will be rounded out in section 4 by the model of the coating interaction.

3. Simplified model of joint drive

Four out of the group of six joints are driven by the miniature brushless DC motors. A three-phase model of electrical part of the motor can be replaced by a transfer function similar to DC motor, Fig.2. R and L are the engine parameters and ω denote the temporary rotating velocity.

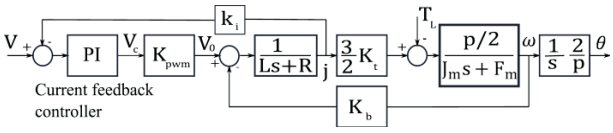

Fig. 2. Simplified engine schema.

The inseparable element of a professional servo-mechanism is a high efficiency PWM power amplifier, with a PI current feedback controller. Besides linearizing properties it allows servo-mechanism to work in a torque control mode. A power amplifier transfer function, binding phase voltage v_0 with control voltage v_c equals

$$\frac{v_0}{v_c} = \frac{K_{PWM}}{1 + sT_{PWM}} \tag{4}$$

The amplification of *PWM* system is dimensionless and does not exceed the value of 20. The time constant T_{PWM} of amplifier depends on the generator working frequency which modulates the current signal. In the designed servomechanism it comes to 20 kHz, which means that the time constant is 50 μsec. The value of time constant of the power amplifier appears insignificant in comparison with the other time parameters, thus it can be omitted. Because of that, the linear model of considered block with amplification coefficient K_{PWM} can be assumed. The motor-amplifier system can be interpreted in particular cases as a voltage controlled torque generator. For $K_i \neq 0$ the decisive influence on the simplified transfer function has a gain introduced to the system by the amplifier and current PI controller

$$I \approx \frac{k_t}{k_i} \left(V_c - \frac{k_b}{K_{PWM} K_p}\, \omega \right) \tag{5}$$

Because the denominator of the second component in brackets has a big value, the generated current depends very little on the rotating frequency. Thus, the dynamics contributed by the electrical part of the motor can be ignored.

4. Effect of the antiseptic coating

The multi-link surgical manipulator is covered by the antiseptic coating, which covers the outer surface of a manipulator and in this way insulates all parts of construction from a human body providing a high sterility. Despite of low thickness, during the fast robot movements (bending and twisting), the coating generates some complex dynamic interactions acting on the joints. The analytical model of coating can be described by Love's equations [6]. They have a great theoretical potential, however, they are not useful enough in practice. Instead, it seems that the better solution is to apply simple FEM model because of its boundary conditions being easy to configure and no restrictions imposed on the external forces.

4.1. The coating model

The applied model has concentrated masses of mass-spring-damping type and rectangular net topology with sixteen-links neighbourhood (Table 1). It ensures realistic behaviour of all kinds of coating deformations.

Table 1. Kind of interactions for perpendicular net.

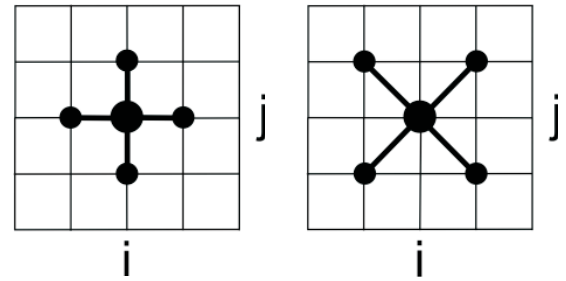

Interactions of type A. *Interactions of type B.*

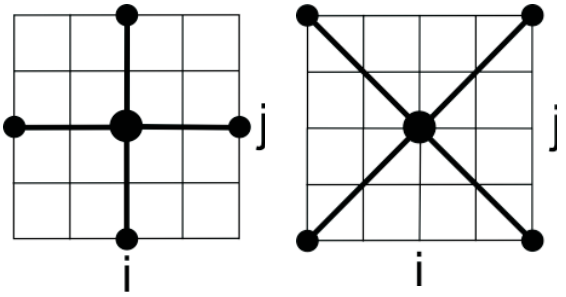

Interactions of type C. *Interactions of type D.*

Interactions of type A - happen between masses in direct contact only in the main directions. These interactions are responsible for stretch deformations. Interactions of type B - occur between masses in direct contact only in the diagonal directions. These interactions are responsible for shearing deformations. Interactions of type C - happen between mass and its far neighbour in the main directions. These interactions are responsible for bending deformations. Interactions of type D - occur between far neighbours in the diagonal directions and improve bending properties of the surface. To obtain the three-dimensional coating equations, we assumed the initial (rest) length of the links are L_{ij}^0. The value of a spring force (three components) between each two points of the net can be obtained from the following equation:

$$F_{ij}^s = k_{ij} \left(\| x_i - x_j \| - L_{ij}^0\right) \frac{x_i - x_j}{\| x_i - x_j \|} \tag{6}$$

where x_i, x_j are the spatial coordinates of point masses, $\| x_i - x_j \|$ - the current length of a link. The force components are proportional to the spring coefficient k_{ij}, and have agreeable directions with the links which are scaled versus current link length. This is expressed by the quotient in equation (6).

In similar way we calculate the friction forces which attenuated the move in a way proportional to the masses velocity (7) with coefficient d_{ij}.

Introduction of a scalar product $(v_i - v_j, x_i - x_j)$ allows describing in a very compact way a projection of friction forces on the spring interactions directions.

$$F_{ij}^d = d_{ij} \left(v_i - v_j, x_i - x_j\right) \frac{x_i - x_j}{\| x_i - x_j \|} \tag{7}$$

In general, both coefficient, k_{ij} and d_{ij}, might depended on the node coordinates. It allows including nonlinear phenomena into the model.

Surrounding and contact interactions are the components of the external forces. The force of such interaction on a node depends on a size of the coating surface (Fig. 3).

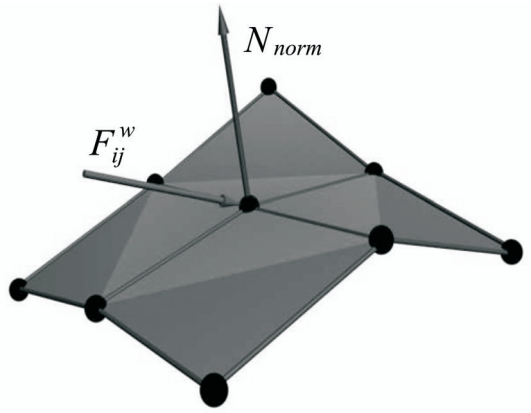

Fig. 3. Normalized vector a medium reaction and the normal to surface in the node.

Normal vector N_{norm} to the surface closed to the nearest node area is equal to the normalized vector calculated as an average from the four normal vectors, determined for the triangles which are adjacent to the node. Finally, the force vector F_{ij}^w acting on the node can be described as:

$$F_{ij}^d = k_w P_{pow} N_{norm} \rho_w \tag{8}$$

where P_{pow} is the shell surface in the node surrounding, ρ_w is the pressure [Pa], generated by the medium on the surface which perpendicular to its direction. The gravity interactions are equal $F_{ij}^g = g m_{ij}$, where $g = [0,0,-9{,}81]^T$.

$$\bar{x}_{ij} = m_{ij}^{-1} \sum_{i=1}^{k} \left(F_{ij}^w + F_{ij}^g - F_{ij}^s + F_{ij}^d\right),\ k = 12 \text{ or } 16 \tag{9}$$

Thus the equations of dynamics for the nodes of surface (9) are applied to obtain the acceleration by the use the Verlet algorithm described in subsection 5.1.

4.2. The free and bounded nodes

In the model of a robot coating, classification on free and bounded nodes has been introduced. Bounded nodes are fixed to some points of an arm and they are used to model clamps. The examples of such nodes are nodes which are located on the first circumference of a cylinder (Fig. 4). The rest of a coating node structure will follow their movements as long as the spring and interaction forces will permit.

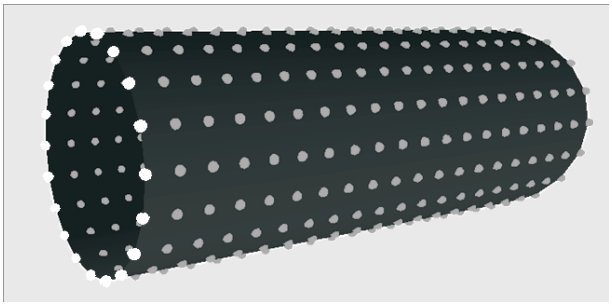

Fig. 4. The free (grey) and bounded (white) nodes on the robot arm surface.

It is enable to act on the any free surface node or on the group of nodes by the vector of forces with different value and direction.

4.3. Coating reaction to joint movement

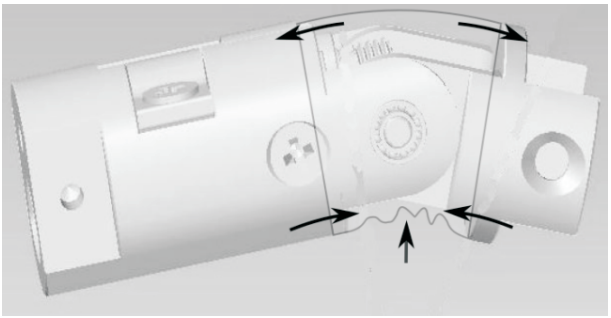

Fig. 5. The coating deformations.

Difficulties in deriving the coating reaction to the joint bending are caused by two phenomena. Firstly, the majority of the coating free nodes are in permanent contact with arm surface and only little part remains free in joint surroundings. It might cause small, but significant longitudinal movement. Secondly, while the joint is bending, the covering coating is influenced by two different deformations. On the one hand it is stretching above the joint and on the other side it is compressed, what is shown in the Fig. 5.

A reaction on compression is difficult to derive because the transversal dislocations of coating are highly probable. It can be assumed that "improbable" transverse deformations (pointed by the vertical arrow in Fig. 5) will introduce a stochastic distribution of stretching moment and a slight amplitude. The stretched fragment acted on the joint with the moment distributed on the radius, which is proportional to local elongation of coating. The interactions are the strongest in the plain of movement and the weakest in the joint axis (Fig. 6). The angle $\beta \in (-90, +90)$, θ_i is a joint angle and R denotes a robot arm radius.

$$F_k \approx k\Delta L_m = kR\sin(\theta_i)\cos(\beta) = 2kR\sin(\theta_i) \tag{8}$$

An elongation of the coating inflicts all four kinds of interactions for a rectangular net described in Table 1.

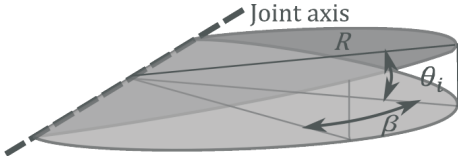

Fig. 6. The local elongation of coating.

In the fourth joint (the rotation around the longitude axis) the coating reactions correspond to the joint twist versus its rotation angle. It has been assumed that this reaction is connected with two layers of free nodes and the reaction force is derived from the equation (10) in a reconfigured form. In this case there are two kinds of interactions: type A and type B, responsible for this reaction forces (in the diagonal directions).

5. Simulation investigations

Joints models together with the coating model constitute resulting simulation structure, which glues together the systems described in subsections 2-4. The block diagram of the hinge joint is shown in Fig. 7.

The dynamical interactions T_L occurring in the joints are the sums of torques generated by the coating and arms

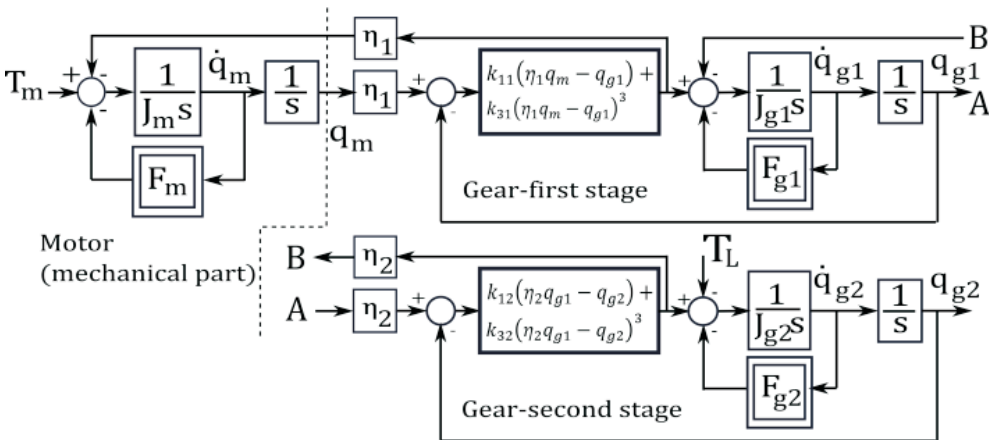

Fig. 7. Block diagram of the joint model.

reactions which are derived from closed models. Because of this, the influence of the reaction of elastic coating can be precisely evaluated and the effects of using the multi-stage planetary gearing can be observed.

5.1. Numerical stability

Because of a big range of coefficients describing the gears and parameters of all the motors (the coefficients of stiffness, friction, inertia etc.), which exceeded to, the equations of motion are ill-conditioned. For assumed tolerance of calculations which was set at 0.01 (1%), despite the use of scaling technique for system variables, the numerical stability was achieved for the step of 0.1 [μs] and Bogacki-Shampine integration method of the third order. Thus, the time of the simulation consumes a lot of time. The coating contains several thousands nodes, conjugated each other, which might to have collisions with the robot construction. Simulation of this system behavior required fast and stable numerical methods. In this work the Verlet algorithm of second order [7] has been applied. It based on performing several operations in the three steps:

$$\begin{cases} x_i(t+\Delta) = x_i(t) + v_i(t)\Delta + \dfrac{a_i(t)\Delta^2}{2} \\ v_i(t+\dfrac{\Delta}{2}) = v_i(t) + \dfrac{a_i(t)\Delta}{2} \qquad \textit{Actualisation } a_i(t+\Delta) \\ v_i(t+\Delta) = v_i(t+\dfrac{\Delta}{2}) + \dfrac{a_i(t+\Delta)\Delta}{2} \end{cases} \tag{9}$$

These steps are as follows:

- calculation of current position $x_i(t+\Delta)$ and velocity $v_i(t+\Delta/2)$ in mid-point,
- calculation of acceleration $a_i(t+\Delta)$ from equation (9)
- updating velocity.

For $\Delta = 10^{-4}$ [s] this method allows to simulate a system with 80x36 nodes in real-time.

5.2. Results of investigations

The aim of performed simulations was to examine the properties of the surgical manipulator joint during its typical movements. The *start-stop* and *forward-reverse* movements with the different characteristic have been tested. Results of the conducted tests are showed below.

In the Fig. 8 time plots of the position, velocity and interactions between the torque of gear and motor are presented. One can observe the difference between an angle position of shaft for the motor and joint. Its maximum value is smaller than $2 \cdot 10^{-3}$ rad which means that the position error is about 0.05-0.08 mm for joints with different length. Considering all joints, it can be stated, that the total error of the angle position is less than assumed and does not exceed 0.3 mm. The phase shift compensation of the motor and the joint angle position as well as the correction of the amplitude angle position must be done by related servomechanism.

It is visible in the Fig. 8 a phase shift between angle position of the motor and the joint and it doesn't exceeded 0.27 rad. It can be seen from the Fig. 9 that for the considered joint some high frequency vibrations appear in the reversion phase of work. They do not influence the changes of the joint position, but they will probably lead to quicker fatigue.

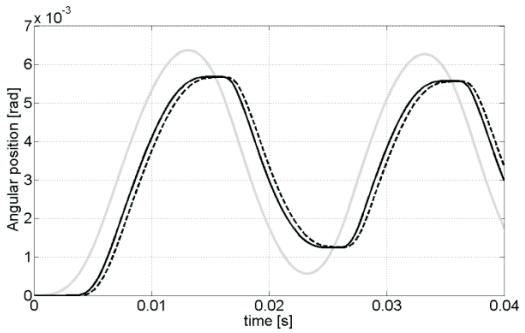

Fig. 8. Time plot of angular positions of the robot joint: motor (gray); one-stage gear (——); joint shaft (------).

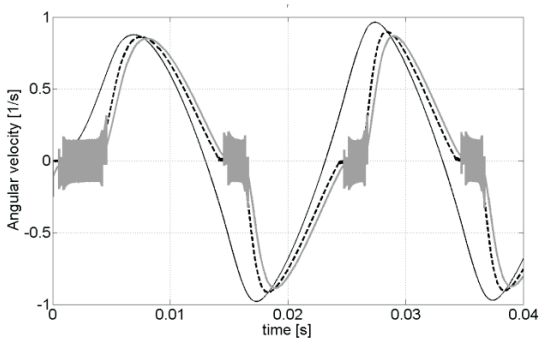

Fig. 9. Time plot of the joint angle velocity; motor (——); one-stage gear (------); joint haft light (gray).

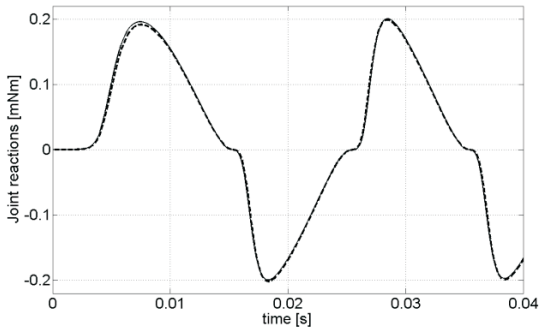

Fig. 10. Time plots of joint reaction on the motor: without coating (——); with coating (------).

The torques of joint reactions on the motor are comprised in the acceptable range and they don't contain high-frequency components with substantial amplitude, Fig. 10. The effect of an elastic coating on the joint can be seen in the zoom (Fig. 11). Observed reactions do not exceed 2% of the motor torque value which ensures the high precision of movements.

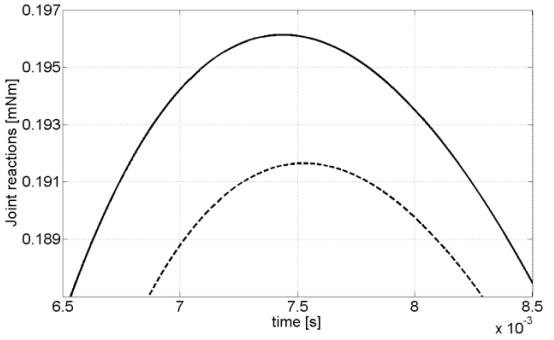

Fig. 11. Zoom of the time plots of joint reaction on the engine: without coating (——); with coating (------).

Performed investigations have crucial importance for the realisation of the next steps essential for the construction and control of the manipulator prototype. The support software is still in development phase and is subject to change. However, the current architecture consists of two parts: a set of s-functions for Matlab/Simulink enviroment, and a component library based on *signals & slots* technology. For visualization and graphic animation of components the OpenGL library is used with some parts of application written in Cg language. As both, the front-end and the back-end of the manipulator software are important parts of the whole project and are still being completed, they will be dealt with in a separate paper.

6. Conclusion

The obtained mathematical model of a multi-link medical robot with an antiseptic coating allows analysing dynamical properties of a considered object with very good reliability. Its structure considers real features of a designed device. The parameters values were evaluated using technical data, which were available from producers of sub-assemblies. The model takes the form of the three-level cascade structure with the blocks containing the nonlinear differential equations. An associated model of an elastic, antiseptic coating is described by FEM model of the "mass-spring-damping" type, with the rectangular net topology and sixteen-neighbour system. This model reproduces all kinds of deformations which influence the working joint with satisfactory realism. Design of the surgical manipulator is unique construction, it contains 6 links with diameter of 8-10 mm and with the length of the modules about 130 mm. It is driven by brushless DC servomotors with planetary and worm gears, for which the total transmission ratio is above 10000:1. Essential feature of this manipulator is an antiseptic coating which covers all the construction. Because of the complicated form of the drive model with three-stage planetary gearings and coating interactions, a control of such system is significantly different from typical industrial robot control. The results of performed simulations show that the value of the phase shift of the shaft angle position versus the joint axis comprise in the range of $\pm 2 \cdot 10^{-3}$ rad and the corresponding velocity amplitude reduction level is about 15%. It means that to achieve a high precision of planed manipulator movements, a compensation of a rotation angle of the motor shaft should be introduced in the process of designing control. Additionally, performed tests assert the presence of high-frequency vibrations in considered system which can be seen in Fig. 9. They have an adverse influence on the joint work and will complicate a control system. Because the manipulator in question is intended to minimally-invasive surgical operations where the precision of movement plays a crucial role, information about main properties of model dynamics are essential for the designing of control system. The appropriate choice of the identification and control algorithms for the derived model allows to suppress the adverse phenomena and to exceed required precision of movements. The performed investigations will be put in practice using the specially constructed laboratory stand with the medical robot prototype which is now under construction.

ACKNOWLEDGMENTS

The research was supported by the Ministry of Science and Higher Education in Poland. Under project No 2376/B/T02/2010/38.

AUTHORS

Ryszard Leniowski* - Department of Computer and Control Engineering, Rzeszów University of Technology Wincentego, Pola 2, 35-959 Rzeszów.
E-mail: lery@prz-rzeszow.pl.
Lucyna Leniowska - Institute of Technology, University of Rzeszów, Rejtana 16A, 35-959 Rzeszów.
E-mail: lleniow@univ.rzeszow.pl.
* Corresponding author

References

[1] J. Cieślik, R. Leniowski, L. Leniowska, "Roboty medyczne nowej generacji - prototyp wieloczłonowego robota chirurgicznego". In: *Proc. of KKR'11*, Karpacz 2010. (in Polish)

[2] R. Pajda, L. Leniowska, R. Leniowski, J. Cieślik, "Projekt wieloczłonowego manipulatora chirurgicznego nowej generacji". In: *Proc. of KKR'11*, Karpacz 2010. (in Polish)

[3] Faulhaber GMBH: Brushless DC-Servomotors. *Technical information*, 2010.

[4] T. Eritenel, R. Parker., "Vibration Modes of a Helical Planetary Gears". In: *Proceedings of the IDETC/CIE 2009*, San Diego, USA, 2009.

[5] H. Olsson, K.J. Aström, "Observer-based friction compensation". In: *Proceedings of the 35th IEEE Conference on Decision and Control*, Kobe, Japan, 1996, pp. 4345-4350.

[6] F. Axisa, P. Trompette, "*Modelling of Mechanical Systems: Structural Elements*", vol. 2, Elsevier 2005.

[7] E. Hairer, C.Lubich, G. Werner, "Geometric numerical integration illustrated by the Stormer-Verlet method", *Acta Numerica*, Cambridge University Press, 2003, pp. 399-450.